Tissue Eng Regen Med (2017) 14(5):539–556
DOI 10.1007/s13770-017-0063-0

Online ISSN 2212-5469
Print ISSN 1738-2696

ORIGINAL ARTICLE

Atelocollagen-based Hydrogels Crosslinked with Oxidised Polysaccharides as Cell Encapsulation Matrix for Engineered Bioactive Stromal Tissue

Andreea Luca[1] · Maria Butnaru[2] · Sergiu Stelian Maier[1] · Laura Knieling[3] · Ovidiu Bredetean[2] · Liliana Verestiuc[2] · Daniela Cristina Dimitriu[3] · Marcel Popa[1]

Received: 18 January 2017 / Revised: 1 June 2017 / Accepted: 5 June 2017 / Published online: 19 September 2017

Abstract Tissue stroma is responsible for extracellular matrix (ECM) formation and secretion of factors that coordinate the behaviour of the surrounding cells through the microenvironment created. It's inability to spontaneously regenerate makes it a good candidate for research studies such as testing various tissue engineered products capable of replacing the stroma in order to assure normal tissue regeneration and function. In this study, a bioactive stroma was obtained considering two main components: 1) the artificial ECM formed using atelocollagen-oxidized polysaccharides hydrogels in which the polysaccharide compound (oxidised gellan or pullulan) has the role of crosslinker and 2) encapsulated stromal cells (dermal fibroblasts, ovarian theca-interstitial and granulosa cells). The cell-hosting ability of the hydrogels is demonstrated by a good diffusion of globular proteins (albumin) while the fibrillar morphology proves to be optimal for cell adhesion. These structural properties and cytocompatibility of the components maintain good cell viability and cell encapsulation for more than 12 days. Nevertheless, the results indicate some differences favouring the gellan crosslinked hydrogels. Ovarian stromal cells functionality was maintained as indicated by hormone secretion, confirming cell–cell signalling in encapsulated and co-culture conditions. *In vivo* implantation shows the regenerative potential of the cell-populated hydrogels as they are integrated into the natural tissue. The possibility of cryopreserving the hydrogel-cell system, while maintaining both cell viability and hydrogel structural integrity underlines the potential of these ready-to-use hydrogels as bioactive stroma for multipurpose tissue regeneration.

Keywords Bioactive engineered stroma · Cell encapsulation · Oxidised polysaccharides

1 Introduction

Stromal tissue plays a key role in sustaining organ function through a microenvironment created by the cooperation between stromal cells and ECM components. It is actively participating in multiple biochemical processes between tissue and blood responses e.g. nutrients exchange, growth factors, cytokines, with an important role in inflammatory response as well as conducting cell behaviour in cancer [1, 2]. Its inability to spontaneously regenerate makes it a good candidate for research studies such as testing various tissue engineered products capable of replacing the stroma in order to assure normal tissue regeneration and function. Obtaining tissue engineered products assumes translating the *in vivo* into *in vitro* by combining natural with synthetic

✉ Maria Butnaru
maria.butnaru@umfiasi.ro

[1] Department of Natural and Synthetic Polymers, Faculty of Chemical Engineering and Environmental Protection, Gheorghe Asachi University from Iasi, Boulevard Profesor Dimitrie Mangeron 67, 700050 Iasi, Romania

[2] Department of Biomedical Sciences, Faculty of Medical Bioengineering, Grigore T. Popa University of Medicine and Pharmacy, Kogalniceanu Street 11-13, 700454 Iasi, Romania

[3] Department of Morphofunctional Sciences, Faculty of Medicine, Grigore T. Popa University of Medicine and Pharmacy, University Street 16, 700115 Iasi, Romania

or modified materials to which the biological component i.e. cells is added. Most biomaterials with tissue engineering applications are in first instance designed, treated by different chemical processes to eliminate the cytotoxic by-products, and then populated with cells [3, 4]. A biomaterial-cell system can be obtained using techniques that involve populating it's surface or creating a sandwich like structure, with cells placed between the two layers of the biomaterial [5–8]. Even though they have the advantage of using a diverse range of components often with a well-defined architecture, these approaches usually result in a non-uniform cell distribution inside the biomaterial.

Obtaining a uniform cell distribution can be done by encapsulating cells into hydrogels. Those hydrogels can mimic the ECM by offering an optimal microenvironment for normal cell functioning, cell–cell interactions, molecule diffusion and ideally by presenting adhesion cues for cells [9]. However, to be able to use this approach in populating the hydrogels with cells, the components that come into direct contact with the living cells have to be very carefully selected.

Hydrogel cell encapsulation usually requires the use of chemical reagents that play a crosslinker role, such as 4S-StarPEG, tetrakis(hydroxymethyl) phosphonium chloride, different enzymes or polymers functionalised with reactive groups e.g. methacrylates, such as gelatin methacrylate [10–14]. The presence of methacrylate moieties usually implies cell exposure to UV light for photocrosslinking, which has its drawbacks. Physical hydrogels obtained based on ionic crosslinking are also used for cell encapsulation yet again, the cells are exposed to different ionic strengths and moreover, the hydrogels usually do not offer a proper microenviroment for cell–cell interactions [15–18].

Oxidised polysaccharides e.g. alginate, dextran, cellulose, gellan, hyaluronic acid, can be used with a double role in hydrogel formation, crosslinker and structural component. Studies have been proven the cytocompatibility of these materials. However, according to Tang et al. [19], in order to be appropriate for cell encapsulation, the oxidation degree of the polysaccharide must not exceed 20% (it was demonstrated that a higher number of aldehyde groups can have cytotoxic effects) [20–31]. This crosslinking method allows hydrogel formation in the presence of cells, without exposing the cells to potentially toxic chemical reagents or irradiation; in addition, the method can be used for stabilising polymers with available amino groups, such as collagen.

Collagen offers numerous advantages such as being the main component of ECM, can form hydrogels in physiological conditions and its high biocompatibility, offering a diversity in terms of being used as a main component in many tissue engineered products [32]. Due to weak mechanical properties as a non-crosslinked material collagen can undergo a crosslinking process in order to enhance its mechanical properties. This crosslinking procedure will affect the cell integrin binding site and therefore the cell activity on the collagen substrates. As alternative collagen can be used as gel for cell encapsulation, accompanied by other natural or modified synthetic polymers in order to obtain chemically crosslinked hydrogels [32–34]. Gellan and pullulan are two linear polysaccharides with properties that recommend them for tissue engineering applications, which can contribute to collagen mechanical improvement. Gellan has gained a lot of interest especially in cartilage tissue engineering [35, 36]. Gellan offers encouraging results in ability to maintain the viability of encapsulated human nasal chondrocytes, rat bone marrow cells or mesenchymal stem cells with [37]. Pullulan's use in tissue engineering applications is directed especially towards cartilage and bone regeneration or as cytoadhesive [38]. An oxidised pullulan/collagen hydrogel has been studied as soft tissue filler, but without cell encapsulation, where the oxidising agent was used also as crosslinker [39, 40]. Other macromolecules or macromolecular blends have also been used for cell encapsulation e.g. Matrigel, alginate, fibrin, hyaluronic acid, peptides or synthetic polymers. Even though Matrigel offers a very complex milieu for encapsulated cells, the tumorigenic origin, uncharacterized growth factors and composition variability are major disadvantages [41, 42]. Unlike alginate and synthetic polymers, collagen offers the advantage of interacting with cells on a molecular level and can be extracted without expensive techniques, as compared to recombinant peptides used for hydrogel formation. The addition of oxidised polysaccharides preserves collagen properties when interacting with cells, while improving its mechanical characteristics, making collagen-oxidized polysaccharides a very attractive option for cell encapsulation.

In addition to their advantages as biocompatible 3-D scaffolds, collagen-based constructs represent an option for obtaining ready-to-use hydrogel-cell systems for immediate use. Thus far, studies were conducted for cryopreserving cells by complex freezing protocols using alginate as an encapsulation matrix, simple or combined with gelatin and fibrinogen and functionalised with RGD tripeptide groups [43–46].

In this paper, a mix of atelocollagen, sodium hyaluronate (NaHyal) and partially oxidised polysaccharides (gellan or pullulan) was investigated for its potential to form hydrogels as an artificial ECM. This novel stromal-like concept facilitates cell macro-encapsulation and cryopreservation. In the obtained tissue engineered construct NaHyal was used as an ECM compound as well as a

cryoprotectant, while oxidised polysaccharides were used as crosslinkers. The functional convenience of the hydrogels we propose, as the structural component of an artificial stroma, was tested on stroma specific cells, respectively *Albino* rabbit primary dermal fibroblasts and ovarian theca-interstitial and granulosa cells.

2 Materials and methods

2.1 Materials

Type I atelocollagen was purchased from StemCell Technologies, at a stock concentration of 6 mg/mL. Low acyl gellan (~300 kDa) was obtained from Kelco and was used at a concentration of 10 mg/mL after solubilizing in double-distilled water, at 80 °C. Pullulan (~100 kDa) was purchased from Fluka and was used at a concentration of 10 mg/mL. Lyophilized collagenase with 220 units/mg activity was purchased from Gibco, Life Technologies. Follicle-stimulating hormone (FSH) and luteinizing hormone (LH) were a kind donation from Merck-Serono Romania. Sodium meta-periodate ($NaIO_4$) was purchased from Merck and ethylene glycol reagent grade, from Fluka. All the other reagents and culture media were purchased from Sigma-Aldrich.

2.2 Polysaccharide oxidation

The polysaccharide oxidation was performed according to the protocols found in the literature and was described in detail in our previous paper [19, 47]. Briefly, a gellan solution was prepared at a concentration of 10 mg/mL by adding the gellan powder in double-distilled water and bringing the mixture at 80 °C for complete solubilisation under magnetic stirring, to avoid gelation. After cooling, while maintaining the stirring, the oxidising process was started by adding 0.1 M $NaIO_4$ dropwise. The whole process was conducted away from direct light exposure. After adding the $NaIO_4$, the mixture was kept for 3 h under mild stirring, after which an equimolar quantity of ethylene glycol relative to that of $NaIO_4$was added to quench the oxidation reaction. This was continued for 30 min. The resulting solution was then dialysed under stirring, for 3 days in doubled-distilled water, in dialysis membranes with a MWCO of 12,000 Da. The water was changed two times daily (three times in the first day) to ensure a good purification of the product. After this, the oxidised polysaccharide was freeze-dried and kept under vacuum, at 4 °C until use. The same protocol was used for the oxidation of pullulan except for the solubilisation step which did not require any heating. The oxidation degree was determined using the titrimetric method with hydroxylamine hydrochloride, yielding the same crosslinking potential for both polysaccharides [19, 47].

2.3 Hydrogel mixture preparation

The formation of atelocollagen-oxidized polysaccharide hydrogels is based on the condensation reaction between the aldehydes formed on the polysaccharide as a consequence of the oxidation process and the amines present in lysine aminoacids found on the atelocollagen macromolecules, resulting in Schiff base formation. New hydrogels based on atelocollagen, NaHyal and oxidised gellan or pullulan were obtained as an artificial extracellular matrix for primary cell embedding. For preparing the hydrogel mixtures, center-well organ culture dishes (60 mm, Falcon) were used. The atelocollagen (6 mg/mL stock solution) was first diluted to a concentration of 3.9 mg/mL with Dulbuecco's Modified Eagle's Medium/Nutrient mixture F12 Ham (DMEM/F12) with L-glutamine, supplemented with 10% fetal bovine serum (FBS) and 1% penicillin/streptomycin/neomycin antibiotic mixture with 100 units penicillin, 0.1 mg streptomycin and 0.25 μg amphotericin/mL (P/S/N), the same culture medium as the one used for culturing the cells to be encapsulated. The diluted atelocollagen solution was neutralised with NaOH 1 M and 40 μL of 10× PBS after which 20 μL of NaHyal (3 mg/mL) and partially oxidised polysaccharide were added. The oxidised gellan solution was prepared at a concentration of 10 mg/mL by dissolving the lyophilized oxidised gellan in double-distilled water and heating to 80 °C. The oxidised pullulan solution was obtained at the same concentration, by dissolving it in double-distilled water at room temperature. Three different hydrogel substrates were prepared, in which the dry mass was maintained constant, while varying the atelocollagen and oxidised polysaccharide quantities. The prepared hydrogel compositions are shown in Table 1.

After all the hydrogel components were added the resulting atelocollagen concentration within the mixture was 3 mg/mL. To allow gelation, the hydrogel mixtures were kept at 37 °C for 20 min.

2.3.1 Elasticity modulus measurements

The texture analyser TA-XT2 Plus (Stable micro systems UK) was used for testing the elasticity of the hydrogels, by using a cylinder of 12 mm diameter and compression speeds of 1 mm/s. The slopes of the stress–strain curves at small deformations were used to calculate an apparent compression modulus. Stress-relaxation measurements on the free and on the confined samples were made on the TA-XT2 instrument, as well. The sample height was 0.8 mm with diameter of 12 mm. An initial fast deformation of

Table 1 Molecular composition of the prepared hydrogels

Sample code	Component mass ratio (aK:NaHyal:GelOx or PulOx)	aK (mg)	NaHyal (mg)	GelOx or PulOx (mg)	Total weight (mg)
r (I)	29.5: 1: 1.5	1.77	0.06	0.09	1.92
r (II)	26: 1: 5	1.56	0.06	0.3	1.92
r (III)	19: 1: 12	1.38	0.06	0.48	1.92

10% at 1 mm/s was kept constant for 60 s. For this analysis the r (II) hydrogel composition was tested.

2.4 Diffusion properties of the crosslinked hydrogels

The diffusion properties of the fully hydrated hydrogels were analysed using a bovine serum albumin solution (BSA) at the physiological concentration of 45 mg/mL, in 20 mM phosphate buffer and 150 mM NaCl (PBS) as a solvent. For the diffusion experiment, the hydrogel was fixed between the recipient and donor compartment of a Franz cell, with BSA solution in the donor compartment and PBS in the recipient compartment. The BSA concentration was measured in both compartments every 5 min for the first hour and every 10 min the next hour, using NanoDrop 1000 spectrophotometer. The temperature was maintained at 37 °C throughout the diffusion process. For determining the diffusion coefficient of BSA through the atelocollagen-polysaccharide hydrogel, Fick's second law of diffusion was used and described as Eqs. (1), (2) and (3):

$$D = \frac{1}{\beta \cdot t} \cdot \ln\left(\frac{C_D^0 - C_R^0}{C_D^t - C_R^t}\right), \frac{m^2}{s} \quad (1)$$

$$\beta = \frac{A}{\delta} \cdot \left(\frac{1}{V_D} + \frac{1}{V_R}\right), \frac{1}{m^2} \quad (2)$$

$$\beta \cdot D \cdot t - \ln\left(\frac{C_D^0 - C_R^0}{C_D^t - C_R^t}\right) = 0 \quad (3)$$

with D global diffusion coefficient, m^2/s, t diffusion time, s; C_D^0 and C_R^0 concentrations of BSA in the donor and recipient compartment of Franz cell, respectively, at time $t = 0$; C_D^t and C_R^t concentrations of BSA in the donor and recipient compartment of the Franz cell, respectively at time t; β—geometrical constant depending on A—aria of the section through which the diffusion takes place (m^2) and δ—*the* thickness of the hydrogel, (m); V_D and V_{R-}—liquid volume from donor and recipient compartment, respectively, m^3.

Considering that the concentration of BSA in the donor and recipient compartments had a non-linear variation, for assessing the diffusion coefficient we isolated the linear domain of the associated sigmoidal curves.

2.5 Cells

The primary animal cells used for encapsulation were *Albino* rabbit dermal fibroblasts and *Wistar* rat ovarian theca-interstitial and granulosa cells. The first cell type was chosen due to its basic role in stromal tissue regeneration while the other two due to their secretory activity, in an attempt to generate a specialised (secretory tissue-like) *in vitro* model. All protocols for cell isolation were performed according to animal welfare requirements and with the approval of Ethical Committee of Grigore T. Popa University of Medicine and Pharmacy of Iasi registered on 13 June 2016 for the submitted research No. PN-III-P2-2.1-PED-2016-1230.

2.5.1 Primary dermal fibroblasts isolation

Albino rabbit dermal fibroblasts were isolated using explant technique according to the widely described method, that provides a homogeneous fibroblast population [48]. Briefly, the tissue—rabbit skin biopsy—was collected under sterile conditions, on ice cold Modified Eagle's Medium (MEM) and Hank's Balanced Salt Solution (HBSS) mixture (1:1 v/v), supplemented with 1% P/S/N. After fat and hypodermis removal, the resulting skin was cut into small pieces (1–2 mm) and the fragments were rested on a 60 mm Petri dish, on a thin layer of FBS to facilitate dermis adherence to the culture plate. MEM supplemented with 15% FBS was then added, the culture medium being changed every other day. After observing the migration of the fibroblasts from the tissue fragments, these were removed and the culture was continued until a sub-confluent cell monolayer was formed. The cells from passage 2 and 3 were used for encapsulation into the hydrogels.

2.5.2 Rat ovarian theca-interstitial and granulosa cell isolation

Rat ovarian theca-interstitial and granulosa cell isolation was performed using 21 days female rat ovaries, according to the protocol described in the literature, with mild modifications [49]. The ovaries were collected under aseptic conditions on ice cold HBSS supplemented with

1% P/S/N and then punctured using 27G syringe needles to release the granulosa cells from the ovarian follicles with an advanced stage oocyte, the resulting cell suspension being collected, centrifuged and cultured until sub-confluent monolayer was formed. The remaining stromal tissue was cut into small fragments and added to a solution of collagenase (0.4%), at 37 °C. After tissue fragments sedimentation, the medium with cell suspension was passed through 70 µm nylon cell strainers and centrifuged. The sediment was cultured in DMEM/F12 medium with L-glutamine, supplemented with 10% FBS and 1% P/S/N until a sub-confluent cell monolayer was reached. A concentration of 2×10^5 cells/mL of each cell type was prepared for the encapsulation procedure. For this, each cell type was removed from the culture flasks using standard trypsinization method [48]. The cells from passage 1 were used for cell encapsulation into the hydrogels.

2.6 Cell encapsulation technique

For the cell encapsulation procedure, the hydrogel composition r (II), with a mass ratio 26: 1: 5 (aK:NaHyal:GelOx or PulOx) was chosen due to its better diffusion properties. First, the hydrogel mixture was formed, according to the method described in Sect. 2.3. A cell suspension of 2×10^5 cells/mL was added just before the partially oxidised polysaccharide, to a final hydrogel volume of 0.5 mL. In order to keep all molecular ratios of the hydrogel compounds, the medium for the initial atelocollagen dilution was adjusted with respect to the volume of cell suspension. The hydrogel mixtures were kept in standard culture condition (37 °C, 5.5% atmospheric CO_2 and 95% humidity) for at least 24 h until further analysis was performed. The culture medium was changed every other day. The resulting series of cell-populated hydrogels used after the cell encapsulation procedure were: I.1—atelocollagen hydrogels crosslinked with oxidised gellan and populated with primary dermal *Albino* rabbit fibroblasts, I.2 atelocollagen hydrogels crosslinked with oxidised pullulann and populated with primary dermal *Albino* rabbit fibroblasts; II.1—atelocollagen hydrogels crosslinked with oxidised gellan and co-populated with primary ovarian theca-interstitial and granulosa cells (1:1), and II.2 atelocollagen hydrogels crosslinked with oxidised pullulan and co-populated with primary ovarian theca-interstitial and granulosa cells (1:1). The strategy of cell-populated hydrogel preparation and the macroscopic aspect of the resulted material after crosslinking reaction are presented in Fig. 1.

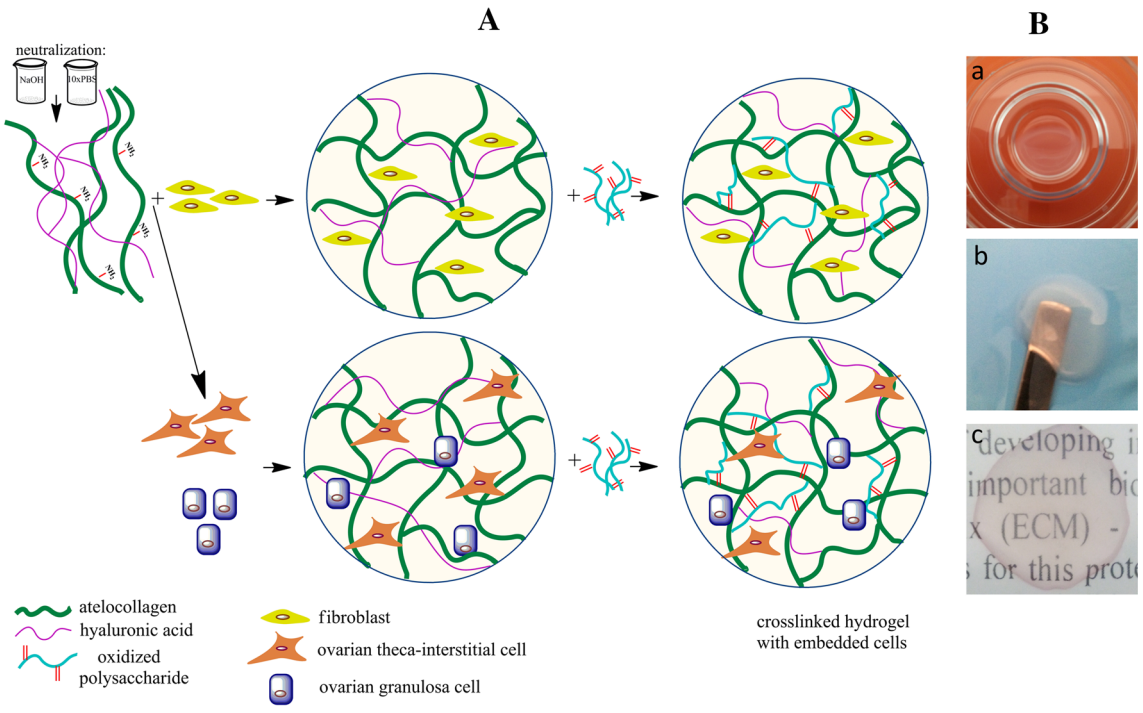

Fig. 1 Schematic illustration of the cell encapsulation steps with the resulting cell-populated hydrogels **A** and macroscopic aspect of the hydrogel **B**

2.7 Cell viability and morphological assessments on the primary dermal fibroblast—populated hydrogels

2.7.1 Light microscopy and fluorescent microscopy

The morphology and cells distribution within hydrogels were assessed in bright field phase contrast microscopy, using a Leica DMI 3000 inverted microscope.

The stained specimens were obtained after chemical fixation of the 3D cultures with 4% paraformaldehyde solution in PBS overnight and double stained with fluorescence blue DAPI (4′,6-diamidino-2-phenylindole) and red Rhodamine-Phalloidin. The hydrogels were washed for several times with PBS, kept for 30 min in 0.5% Triton X-100 solution for cell membrane permeabilization, washed again with PBS and then stained. Hydrogels were stained first with 50 ng/mL Rhodamine-Phalloidin solution in PBS for 2 h and then with 5 μM DAPI for 30 min. The blue fluorescence of the cell nuclei was detected using 358/461 nm excitation/emission filter while actin cytoskeleton was highlighted using 540/565 nm excitation/emission filter.

The histological analysis of the hydrogel structure was performed on the 10% formaldehyde fixed hydrogels that were dehydrated, embedded in the paraffin blocks, sliced and then stained using haematoxylin and eosin (H&E) technique, according to the usual standard protocols. Briefly, the hydrogels were washed for several times in HBSS solution, and then immersed in 10% formaldehyde solution in HBSS for 48 h. Fixed hydrogels were dehydrated in one of the most frequently used graded series of alcohols (35, 50, 70, 95 and 100%). The embedding of the hydrogels in paraffin blocks was performed after their clearing in repeated xylene and toluene baths. All post-fixation procedures were performed using the automatic system Biooptica CD1000 and sliced using the microtome Leica RM 2235. The tissue samples were stained using H&E technique, according to the standard protocol set by Leica autostainer XL.

2.7.2 SEM analysis

The crosslinked hydrogels with and without the encapsulated primary fibroblasts were analysed by SEM. In order to maintain the morphology of the hydrogels close to wet condition, the hydrogels were dried using critical point drying technique. For this, the hydrogels were fixed in 2% glutaraldehyde overnight and gradually dehydrated in baths of ethanol at increasing concentrations (70, 80, 90 and 3 × 100%). After dehydration, the hydrogels were dried to critical point using EMS 850 Critical Point Dryer. Dehydrated hydrogels were sputter coated with a 30 nm layer of gold and visualised by a scanning electron microscope (Tescan Vega II SBH) at an accelerating voltage of 30 kV. The porosity degree of the two types of dried hydrogels was analysed with ImageJ 1.49 v with Analyse plugin installed, based on the obtained SEM images and was expressed as percent porosity of the analysed area. For this, the images were binarized with the use of threshold command of ImageJ, the black areas of the resulting images representing the pore areas. The area of the pores was calculated in pixel values with the use of the command *Analyse-Measure*. The porosity was determined by calculating the ratio between pore area and total bidimensional area, five different images being analysed for each hydrogel [50–52].

2.7.3 Live/dead cell evaluation of the encapsulated cells

The cell survival rate in the hydrogels was assessed using the live/dead double staining kit which is based on the ability of the live cells to fluorescence in green due to acetoxymethyl ester hydrolysis of the calcein-AM to calcein by intracellular esterases of the living cells, while the nuclei of the dead cells are stained in red by propidium iodide as it passes through degraded cell membranes. The live/dead staining was performed on the hydrogels after 48 h, 5, 7 and 10 days of fresh or frozen 3D culture. Briefly, the cell-populated hydrogels were washed several times in HBSS and stained for 40 min at 37 °C with live/dead fluorescent dye mix, according to the kit protocol. Green fluorescence of the live cells and red fluorescence of the dead cells were visualised with a Leica DM5500Q fluorescent microscope. Percent viability was determined on the fluorescent images by analysing the number of cells stained in green and red, using ImageJ software. For each type of hydrogel, cell viability was calculated as the ratio of green cells to the total number of cells (green and red).

2.7.4 Cell viability and cell proliferation assessing

Cell viability and proliferation capacity of the encapsulated cells was analysed using Alamar Blue® assay (Bio-Rad, AbD Serotec, U.K) based on blue resazurin conversion to pink resorufin by the intracellular reductase activity of live cells. For this, the culture medium from each cell-populated hydrogel was replaced with 300 μL of 10% Alamar Blue solution in DMEM culture media without phenol red and 4 h later the medium was collected and the absorbance of the resorufin was measured at 570 and 620 nm (as reference) using Tecan plate reader (Sunrise model, Tecan Austria GmbH, adapted with Magellan V7.1SP1 software). The assay was performed for the same sample at 24 h, 3, 5, 7 and 12 days of 3D culture, in triplicate. The absorbance

of the resorufin was considered an indicator of cell proliferation.

2.8 *In vivo* performance of the fibroblast-populated hydrogels

The *in vivo* behaviour of the cell-populated hydrogels was analysed on the fibroblast-populated samples, 24 h after cell encapsulation (according to the encapsulation procedure described in Sect. 2.6).

The *in vivo* experiments were performed on *Wistar* rats, according to ISO 10993-2—animal welfare requirements, to ethical regulations and with the approval of the Ethics Committee of Grigore T. Popa University of Medicine and Pharmacy of Iasi registered on 13 June 2016 and mentioned in Sect. 2.5.

All surgical procedures were done under thiopental anaesthesia. An insertion area was prepared on the right flank of the animal, by removing the hair and disinfecting the tegument with a topical solution (Betadine). An incision and a surgically created pocket were made between the hypodermis and dermis (with an approximate diameter of 1.5 cm) for inserting the prepared hydrogels. The incision was closed with surgical nylon suture. After 2, 5 and 7 days the implanted hydrogels and adjacent tissue were removed and prepared for histological analysis following formaldehyde fixation for 48 h in 10% formaldehyde solution in HBSS. Paraffin embedding was done using the automatic system Biooptica CD1000 and the staining with H&E and Masson's trichrome followed the protocols set by the automatic Leica autostainer XL.

2.9 Hydrogel model for cell secretory capacity and cell signalling assessment

Secretory function of the cells and intercellular signalling capacity was determined by estradiol measurements in the culture media in which co-encapsulated theca-interstitial and granulosa cells were cultured. For this, the primary isolated theca-interstitial and granulosa cells that reached sub-confluency (Sect. 2.5.2) were further grown in serum-free DMEM/F12 medium, supplemented with ITS (insulin/transferrin/selenium 5 µg/5 µg/5 ng/mL) and 1 mg/mL BSA. After the cells reached confluence, a suspension mix of theca-interstitial and granulosa cells (1:1) was encapsulated at a final density of 2×10^5 cells/mL (1×10^5 cells/hydrogel) and then cultured in DMEM/F12 medium supplemented with ITS, 1 mg/mL, BSA and 2.5 I.U. LH and FSH for the initiation of steroid hormone secretion. The medium was fully collected for analysis after 48 h of culture, replaced with fresh medium with the same composition and collected again after another 72 h of culture (5 days post-encapsulation). Estradiol detection in the collected medium was done using chemiluminescent competitive immunoassay and Immulite Estradiol kit. Briefly, the method consists in incubation of the samples with a solid phase (beads) coated with polyclonal rabbit anti-estradiol antibody and enzymatic substrate for 60 min, followed by solid phase washing in order to remove the unbounded compounds. Subsequently, the addition of chemiluminescent substrate was made. Chemiluminescent signal was detected with Immulite 1000 immunoluminescent analyser (Siemens). As a control, the collected medium from the same density of cells, cultured in standard 2-D culture system (in the same culture medium), was analysed.

2.10 Cryopreservation of the cell-populated hydrogels

The ability of the atelocollagen hydrogels crosslinked with partially oxidized polysaccharides to preserve cell viability after a freeze-thawing process was analysed for encapsulated fibroblasts after 48 h, on day 5, day 7 and day 10. 10% DMSO in FBS was used as cryopreservation medium and the viability of cryopreserved hydrogel encapsulated cells was compared with the same fresh systems. The freezing of the cell-populated hydrogels was performed following a widely used slow freezing procedure applied to cell culture, using a double-well Mr Frosty freezing box. Before freezing, the culture medium was removed, replaced with the cryoprotectant and left for 10 min in a center-well plate in which the encapsulation was done. After 10 min the culture plate with the hydrogel was sealed and frozen in a low-freezer, at -85 °C. The rapid thawing procedure was performed after three weeks of cryopreservation. After thawing at 37 °C the cryoprotectant was removed and extensively washed with HBSS and culture media, following the culture in the original conditions. Live/dead assay was performed after thawing as it was described in Sect. 2.7.3 and compared to the fresh systems.

3 Results

3.1 Hydrogel mechanical properties and morphology

3.1.1 Macroscopic analysis and mechanical properties

In this study we have obtained new hydrogels having atelocollagen, oxidised polysaccharides and sodium hyaluronate as components, used as an artificial stroma for the encapsulated cells. As a result of crosslinking the atelocollagen with partial oxidised gellan and pulullan, transparent hydrogels with a uniform aspect were obtained. The

Table 2 The elastic moduli of the r (II) hydrogels

Crosslinking agent	Component mass ratio (aK:NaHyal:GelOx or PulOx)	Elastic modulus (Pa)
GelOx	26: 1: 5	61.64 ± 5.42
PulOx		180.95 ± 10.95

r (II) composition was chosen for cell encapsulation due to its mechanical and handling properties (Fig. 1B). The elastic moduli of the hydrogels with r (II) composition are presented in Table 2.

The data presented in Table 2 shows that the nature of the polysaccharide influences the hydrogels elasticity, most probably by creating shorter or larger distances between junctions zones and by increasing the number of crosslinking points (in the case of pullulan-crosslinked hydrogels).

3.1.2 SEM analysis

The microscopic analysis of the hydrogels crosslinked with partially oxidised polysaccharides displayed a porous fibrous structure, influenced mostly by the atelocollagen which is their main component (Fig. 2).

In Fig. 2, it can be noted a regular fibrous structure with small pore sizes resulting from the network of collagen fibres. After analysing the obtained images for the r (II) hydrogel samples, we obtained a porosity of 62.6% for gellan crosslinked hydrogels and of 65.8% for pullulan crosslinked ones. Even if the porous architecture of the hydrogel was better preserved by critical point drying conditions (as opposed to lyophilisation), the dehydration process can influence the actual pore sizes compared to that of the wet hydrogels. The smaller pullulan molecules (compared to gellan), are able to better reach the reactive groups on atelocollagen still, the two types of hydrogels present a quite similar porosity degree.

3.2 The diffusion properties of the oxidised polysaccharide-crosslinked hydrogels

The diffusion properties of the fully hydrated hydrogels were studied on low-molecular-weight albumin (66.21 kDa), which represents an important nutritive, regulatory and protective molecule of the blood serum as well as of the culture media. At physiological pH (7.4) albumin has an anionic charge. This is why the interactions with the hydrogel should be minimal considering that at this pH the atelocollagen has a low positive charge, while the polysaccharides exhibit a strong negative charge. As a consequence, the diffusion will primarily depend on the structure of the fully hydrated hydrogel. We found that albumin diffusion through all hydrogel samples starts in the first 10 min after albumin solution was added in the donor compartment, and lasts for at least 2 h (Fig. 3). Based on the diffusion curves presented in Fig. 3, we concluded that the crosslinker ratio in the hydrogel composition is the main factor that influences the diffusion progress. The numeric values of diffusion coefficients are summarised in

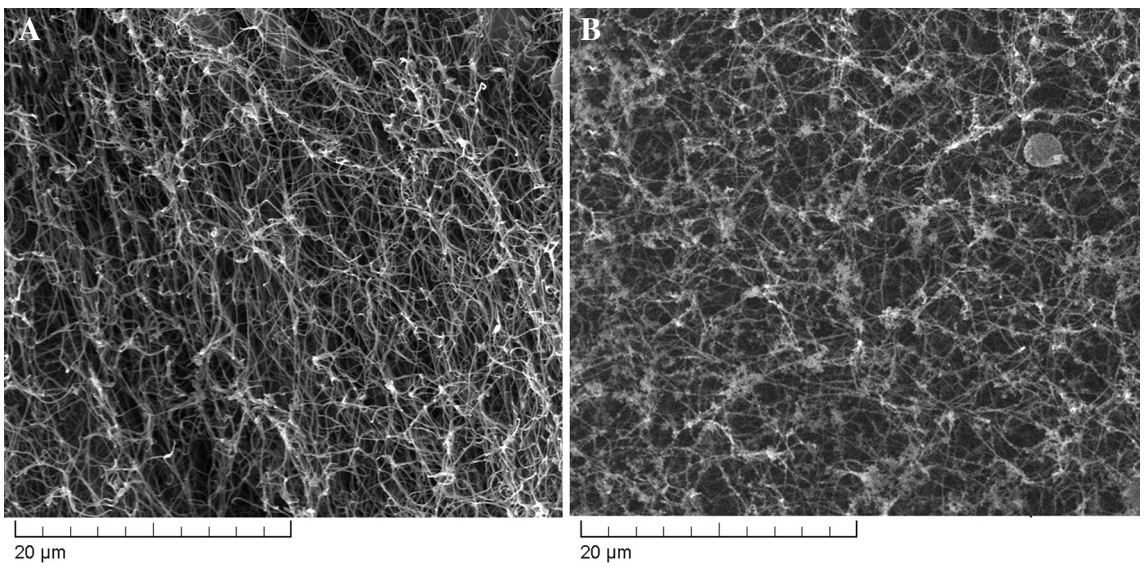

Fig. 2 SEM images of hydrogels dried at critical point (**A** gellan-crosslinked hydrogel; **B** pullulan-crosslinked hydrogel)

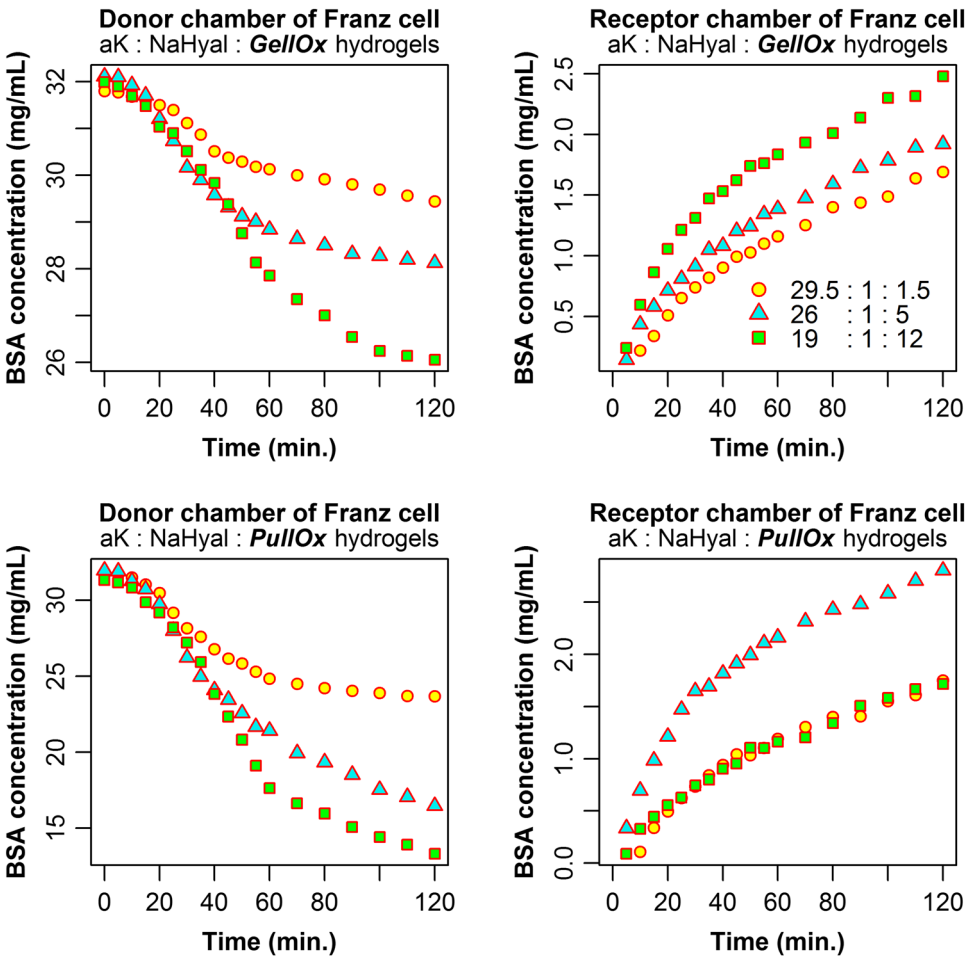

Fig. 3 Diffusion properties of the atelocollagen-based hydrogels crosslinked with oxidised polysaccharides, by means of BSA

Table 3 together with the derived diffusivity characteristics of the investigated hydrogels.

Based on these results the biological performances of the hydrogels were carried out for the r (II) composition.

3.3 Cell viability and morphological assessments on the primary dermal fibroblast—populated hydrogels

3.3.1 Morphological analysis of the cell-populated 3D culture systems

An important aim of regenerative medicine is to achieve an appropriate and efficient way for soft tissue regeneration which often consists of a large compartment of the fibroblast-rich stroma. Using atelocollagen-based hydrogels supplemented with NaHyal and entrapped primary fibroblasts we obtained a soft and flexible 3D cell-populated matrix, transparent, with even cell distribution and elongated cell morphology (fibroblast-like) on the entire hydrogel thickness (Fig. 4).

The dehydrated fibroblast-populated hydrogel structure observed on SEM images (Fig. 5) revealed a relatively dense collagen network which provides a uniform porous scaffold for the entrapped cells.

Histological analysis of the oxidised polysaccharide-crosslinked hydrogels populated with fibroblasts revealed that cells embedded in the gellan-crosslinked hydrogels had a more elongated shape compared to the same cells in the pullulan-crosslinked hydrogels (Fig. 6).

In both gellan-crosslinked and pullulan-crosslinked hydrogels, cell divisions can be noted. The difference between the two hydrogels could be correlated with a higher superficial contraction observed on the pullulan-crosslinked samples and higher stiffness which in turn could be explained by smaller pullulan molecules that are able to better reach the reactive molecules on atelocollagen influencing the cell adhesion microenvironment.

3.3.2 Cell viability assessment

Live/dead assay on both polysaccharide-crosslinked fibroblast-populated hydrogels after 48 h and 5 days of

Table 3 Diffusion coefficients of BSA, overall mass transfer resistance, and the penetration distance through the hydrogel

Sample code	Crosslinker	Diffusion coefficient (m^2/s)	Global coefficient of resistance to mass transfer (s/m)	Coefficient of penetration distance through hydrogel [m ($s^{-0.5}$)]
r (I)	GelOx	4.2718×10^{-13}	4.6819×10^{9}	1.3072×10^{-6}
	PulOx	4.9733×10^{-13}	4.0215×10^{9}	1.4104×10^{-6}
r (II)	GelOx	5.4248×10^{-13}	3.8667×10^{9}	1.4731×10^{-6}
	PulOx	7.2714×10^{-13}	2.7505×10^{9}	1.7055×10^{-6}
r (III)	GelOx	1.0510×10^{-12}	1.9030×10^{9}	2.0504×10^{-6}
	PulOx	1.4505×10^{-12}	1.3788×10^{9}	2.4087×10^{-6}

culture reveals a large number of living cells (in green) compared to non-viable cells (in red) (Fig. 7).

It was determined that viable cell ratio was higher for gellan crosslinked hydrogels both, on day 2 and day 5 as it was presented in Table 4.

The viability and proliferation of the fibroblasts in the hydrogel scaffold were dynamically analysed for a longer period of time. It was found that both gellan and pululan-crosslinked hydrogels support cell viability for at least 12 days with no significant differences between the two of them (Fig. 8).

From the cell evolution graph, it can be noted that the cell division process in both types of hydrogels occurs until day 5, with an exponential growth until day 3 of culture. Thus, according to the absorbance data obtained from Alamar Blue assay, in day 5 there was a threefold increase in the percentage of reduction of resazurin compared to day 1 (about 5% after 24 h of culture and 15% after day 5).

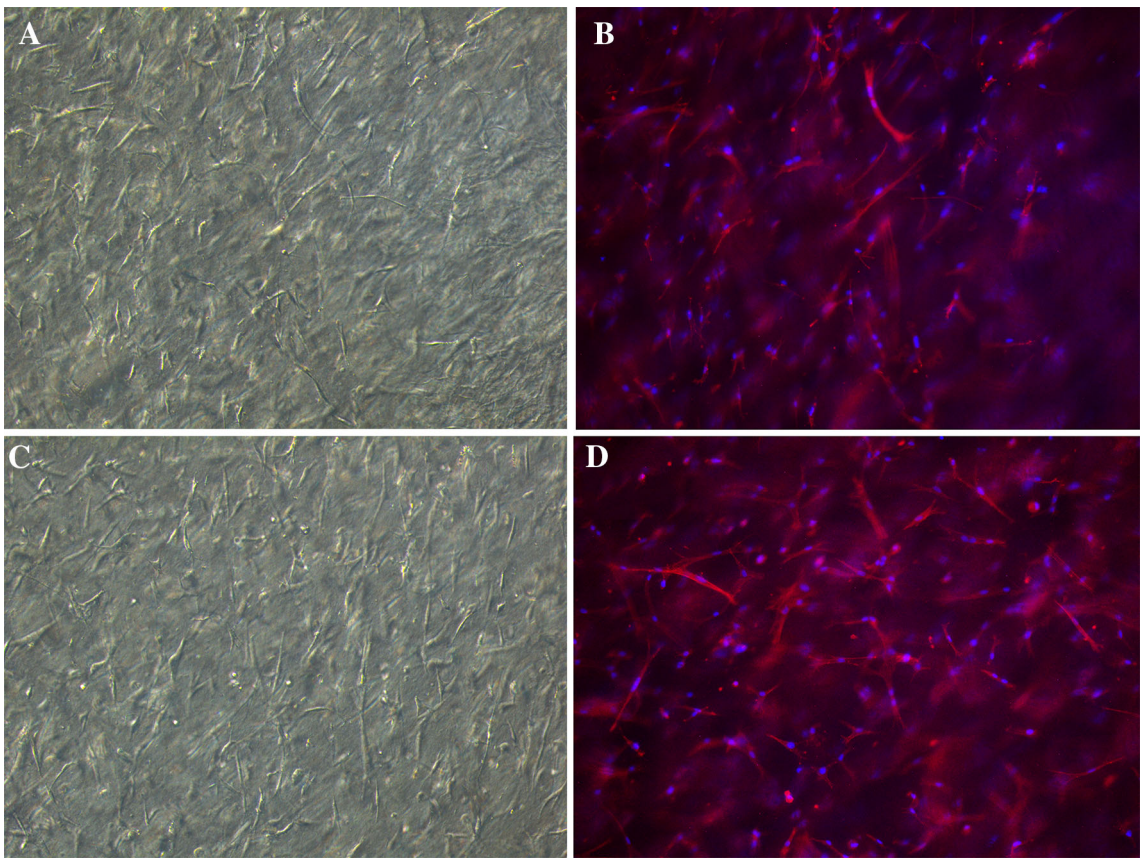

Fig. 4 Microscopic images of the encapsulated cells in gellan-crosslinked hydrogel (**A** bright field; **B** DAPI and phalloidin-rhodamine staining) and pullulan-crosslinked hydrogel (**C** bright field; **D** DAPI and phalloidin-rhodamine staining), 10× objective magnification

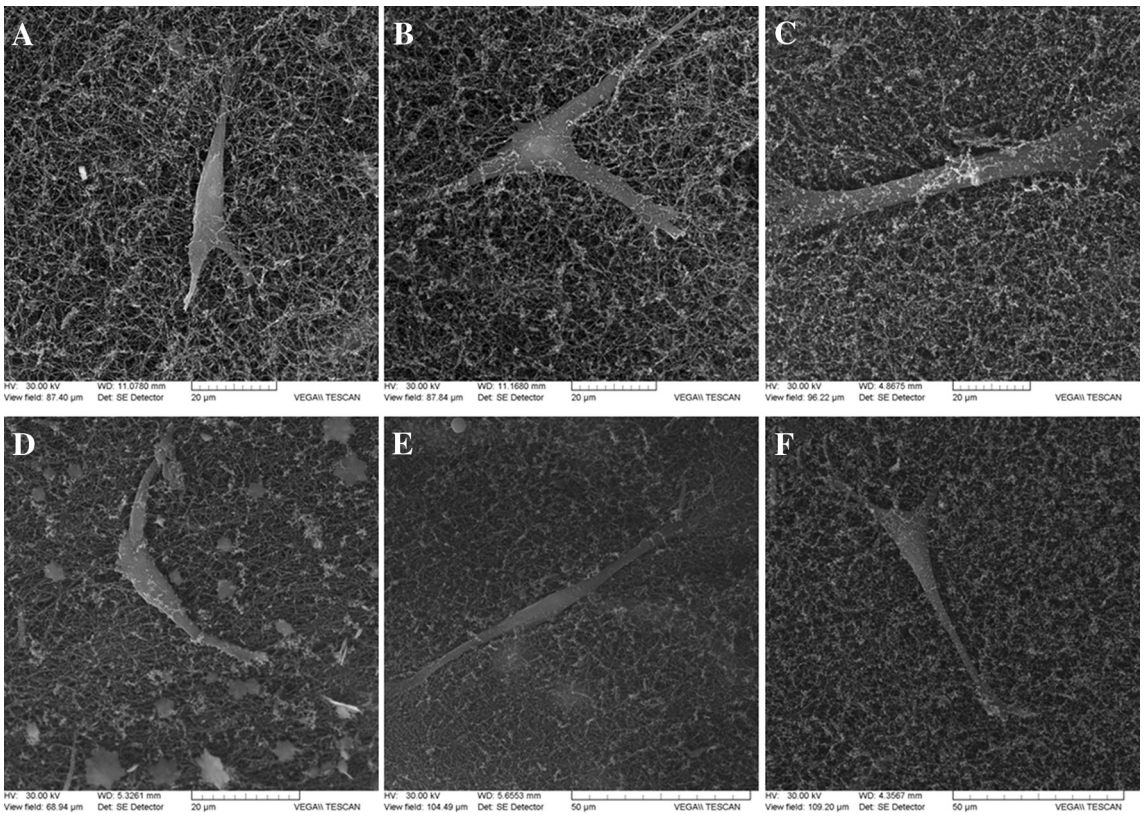

Fig. 5 SEM imagess of the cell-populated hydrogels dried at critical point (**A–C** gellan-crosslinked hydrogels; **D–F** pullulan-crosslinked hydrogels)

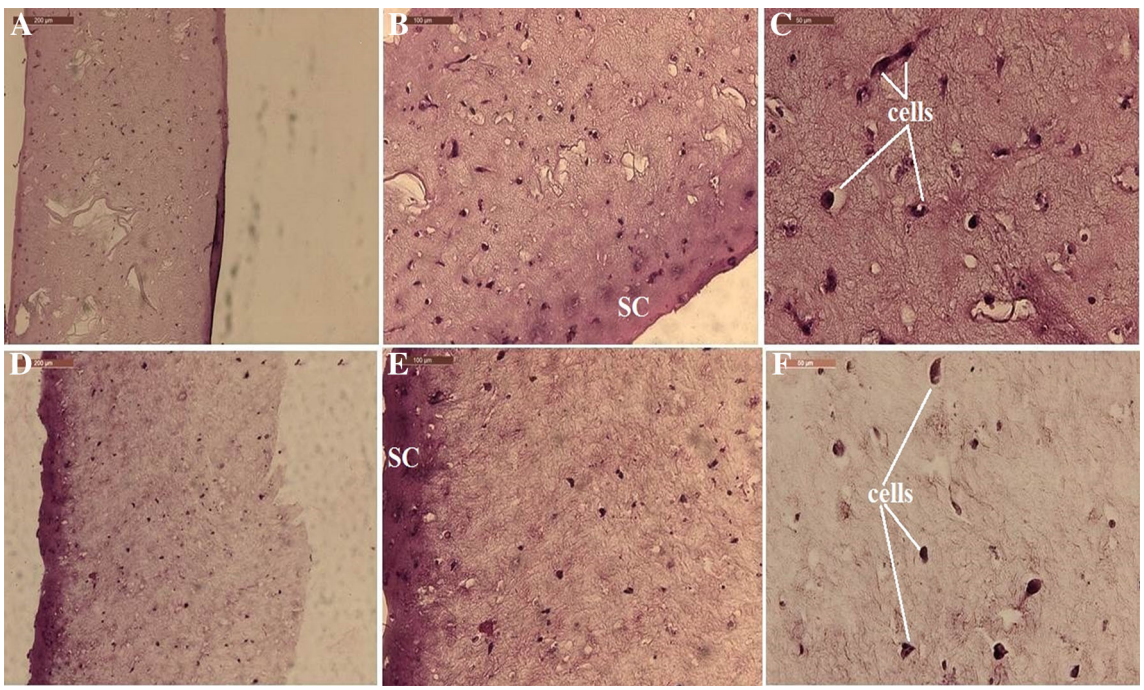

Fig. 6 Microscopic images of stained histological sections of the hydrogels populated with primary fibroblasts (**A–C** gellan-crosslinked hydrogels at 10×, 20× and 40× objective magnifications; **D–F** pullulan-crosslinked hydrogels at the 10×, 20× and 40× objective magnifications). *SC* surface contraction of the hydrogel

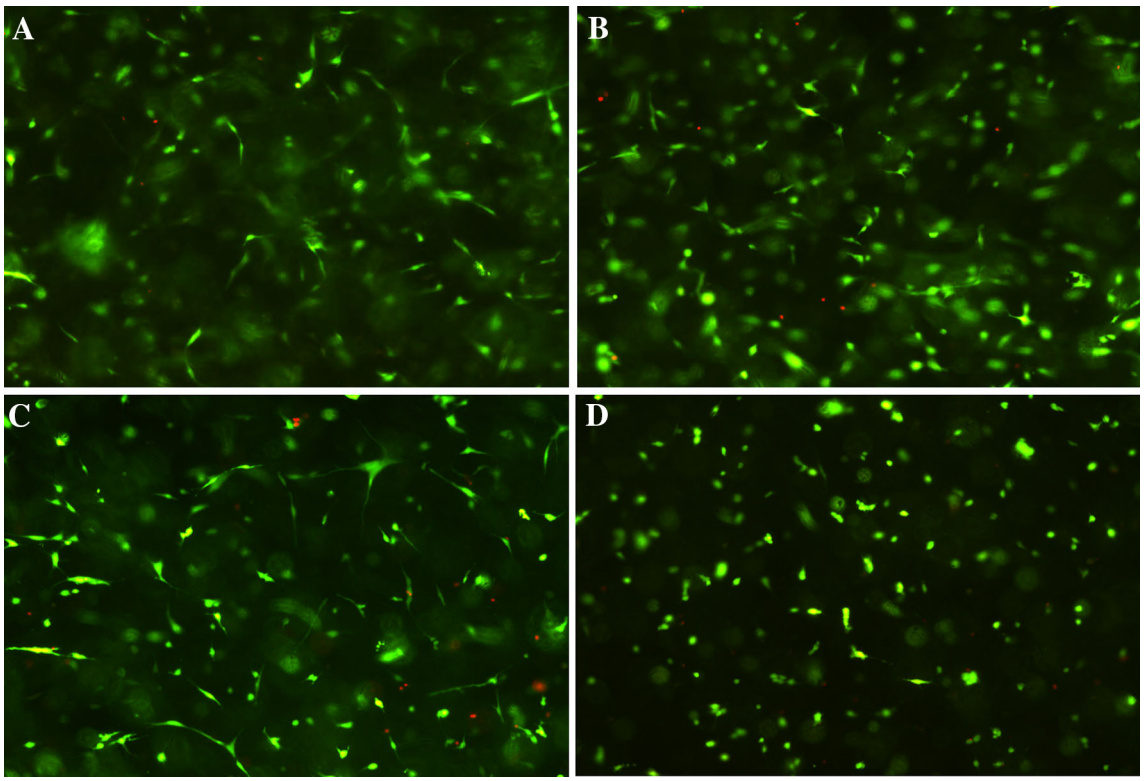

Fig. 7 Live/dead assay on cells embedded in gellan-crosslinked hydrogels (**A** 2 day culture; **B** 5 day culture) and pullulan-crosslinked hydrogels (**C** 2 day culture; **D** 5 day culture) (10× objective magnification)

Table 4 Cell viability in the hydrogels after 2 and 5 days of encapsulation, calculated based on live/dead cell counting

Days of culture (days)	Cell viability (%)	
	GelOx crosslinked hydrogel (%)	PulOx crosslinked hydrogel (%)
2	90 ± 1.6	88.9 ± 1.1
5	85.8 ± 0.14	84.7 ± 1.2

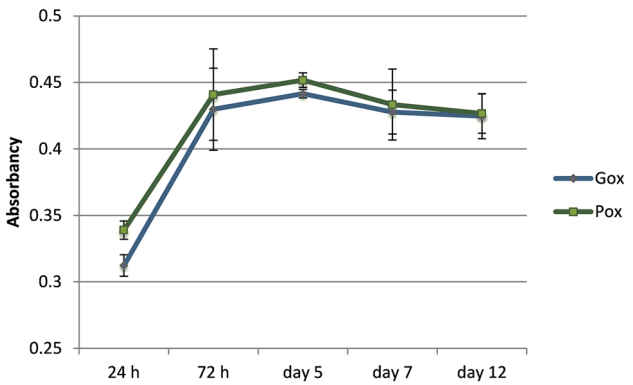

Fig. 8 Alamar-Blue assay on cells embedded in the oxidised polysaccharides-crosslinked hydrogels

3.4 *In vivo* subcutaneous implant analysis of the fibroblast-populated hydrogels

Taking into consideration the *in vitro* analysis results obtained for r (II) hydrogels (aK:NaHyal:GelOx or PulOx 26: 1: 5), the sample crosslinked with oxidised gellan was chosen for the *in vivo* study. The histological analysis of the subcutaneously implanted hydrogels after 2, 5 and 7 days of implantation was performed on H&E stained samples (Fig. 9).

The Masson's trichrome stained samples revealed the collagenous nature of the hydrogel with a structure very close to that of the surrounding host tissue. Large regions of host cells ingrowth (proving the pro-active action of the

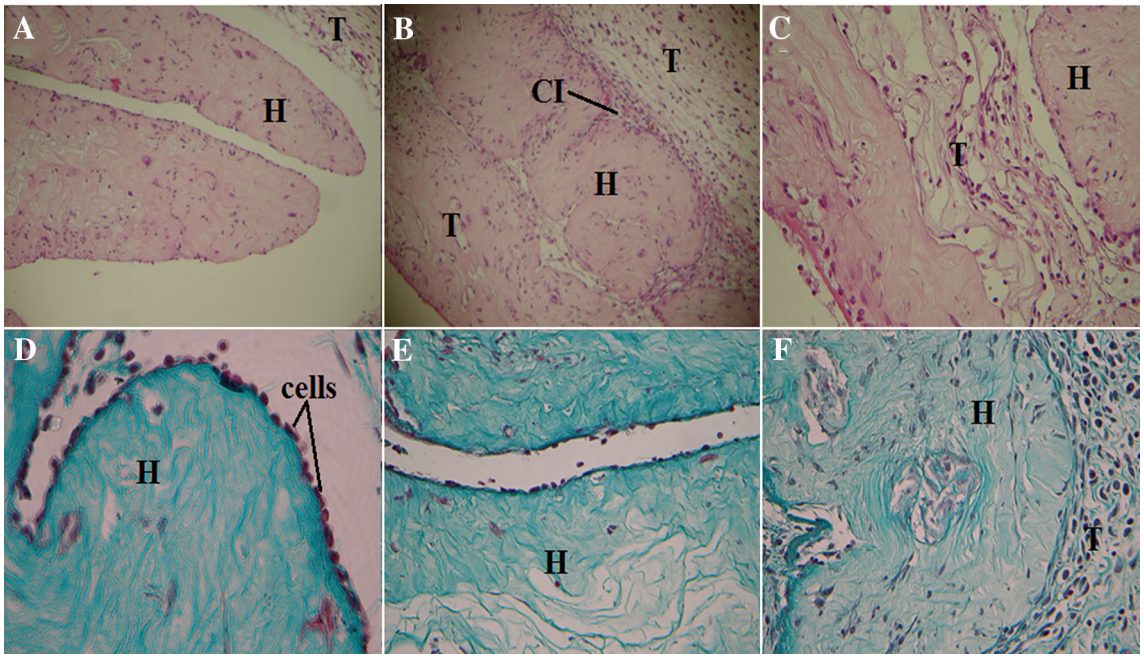

Fig. 9 Microscopic images of the stained histological sections made on subcutaneous implants of cell-populated hydrogels crosslinked with oxidised gellan (**A–C** H&E staining; **D–F** tricrom-masson staining) at 10× and 20× objective magnification. *H* hydrogel; *T* host animal tissue; *CI* cell ingrowth

growth factors secreted by the encapsulated cells), on the hydrogel samples, were detected 5 and 7 days after insertion. A dense layer of large-nucleated cells that are spotted at the hydrogel-host tissue interface suggest a local broad cell proliferation. Cell proliferation into the implanted hydrogel samples (from day 2 to 7 day), shows that the implanted hydrogels are highly biocompatible and have the ability to be quickly remodelled through cooperation between the encapsulated inner cells and those from the surrounding host tissues.

3.5 Secretory capacity and intercellular signalling of theca-interstitial and granulosa cells co-populated hydrogels

An experimental model for functional evaluation of the cell-populated hydrogels was set for gellan/pullulan-crosslinked hydrogels co-populated with ovarian theca-interstitial and granulosa cells.

The estradiol production, quantified after 2 and 5 days of 3D co-culture of the theca-interstitial and granulosa cells in FBS-free medium (Table 5), was quite constant and did not differ between the two groups of hydrogels. Moreover, the estradiol values measured in the 3D cultures were comparable to the 2D control cultures.

The small variation between the two estradiol measurements (day 2 and day 5) indicates that the encapsulated cells maintain their specific functional activity for a long period of time. Estradiol measurements showed that both oxidised polysaccharides are able to form hydrogels that allow hormones diffusion and intercellular communication through cell signalling mechanisms.

3.6 Preliminary data on cryopreservation of the encapsulated cells

The opportunity to store cell-populated hydrogels can offer numerous advantages in regenerative medicine applications. Since tissue engineered products have to be ready to use when needed, the cryopreservation of cells encapsulated in hydrogels has been investigated especially for insulin secreting cells. Different results between slow-

Table 5 17 β-estradiol concentrations determined into the culture media after 2 and 5 days of co-culture of the encapsulated theca-interstitial and granulosa cells

Days of culture (days)	Control (2D cell co-culture) (pg/mL)	GelOx crosslinked hydrogel (pg/mL)	PulOx crosslinked hydrogel (pg/mL)
2	23.92 ± 2.12	25.43 ± 3.14	23.92 ± 4.18
5	24.63 ± 1.16	26.34 ± 2.12	24.24 ± 2.16

Table 6 Cell viability in the fresh and thawed hydrogels after 2, 5, 7 and 10 days of culture, calculated based on live/dead cell counting

Days of culture (days)	Cell viability in fresh and thawed hydrogels (%)	
	Fresh	Thawed
2	90.02 ± 1.63	82.97 ± 2.97
5	85.86 ± 0.14	78.8 ± 2.8
7	86.42 ± 2.16	86.06 ± 1.8
10	90.25 ± 4.9	80.48 ± 2.76

freezing and vitrification, cryopreservation of adherent cells or cell suspensions were reported for hydrogels having the cryoprotectant as a component of the hydrogel [45, 46, 53]. Cryopreservation of adherent cells can provide some advantages in terms of survival rate and stem cell marker expression [54]. In case of the gellan/pullulan-crosslinked hydrogels discussed in this paper, cell viability was maintain over 80% even 10 days after thawing, the results being comparable to fresh cell-hydrogel systems (Table 6; Fig. 10).

4 Discussion

The stromal compound of the tissue has both structural and modulatory role and controls the parenchymal components' behaviour. Stromal tissue can be substituted with ECM-mimicking tissue engineered products having both macromolecular configuration and specific cellular components. Even though numerous studies approach the two components, only few of them have underlined the role of the stromal tissue as a functional support of the parenchyma.

The formation of atelocollagen-oxidized polysaccharide hydrogels is based on the condensation reaction between the aldehydes formed on the polysaccharide (as a consequence of the oxidation process), and the amines present in lysine amino acids found in atelocollagen macromolecules, resulting in Schiff base formation. New hydrogels based on altelocollagen, NaHyal and oxidised gellan or pullulan were obtained (Fig. 1) as an artificial extracellular matrix with porous and fibrillar structure (Fig. 2).

The elastic moduli determined for r (II) hydrogel compositions are consistent with the elastic moduli specific for soft tissues which, according to published data, can vary between 180 Pa for brain, 200 Pa for non-mineralized mesodermal tissues, 0.3–5 kPa for nucleus pulpous cells ECM, to values over 30 kPa for bone [55–57]. Other hydrogels that are usually used for cell encapsulation have been reported to have various elastic modules, like 0.2 kPa for Matrigel, 3.6 ± 0.5 kPa for 0.5% alginate, 0.5 ± 0.1 kPa for fibrinogen/thrombin 25 mg/ml, 1.5 ± 0.3 kPa for 1% hyaluronic acid, 1.3 ± 0.17 kPa for 5% polyacrylamide gels, 0.5 ± 0.2 kPa for 5% PEGDA gels [58]. From Table 2 it can be observed that the hydrogels we have obtained have the elastic modulus in the same range as Matrigel, but without presenting the disadvantages previously pointed out, while the other hydrogels are more rigid.

Regarding to diffusion properties of the designed hydrogels, according to data shown in Table 3, a faster diffusion was observed for r (II) hydrogel, prepared using a composition ratio of 26: 1: 5 (aK: NaHyal: GelOx or

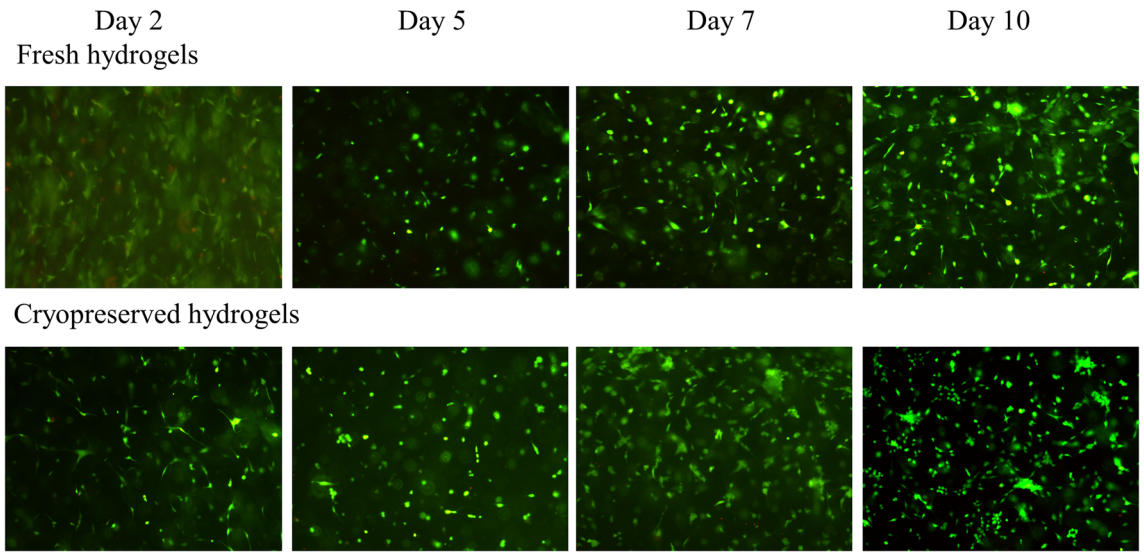

Fig. 10 Live/dead images of the fresh and cryopreserved cell populated hydrogels at day 2, 5, 7 and 10 after encapsulation (10× objective magnification)

PulOx). Even if diffusion through r (II) hydrogels is high, it is slower with more than one order of magnitude as compared with the diffusion of BSA in water (5.9×10^{-11} m^2/s) [59] fact which can be explained by the delay induced due to the entanglement of the macromolecular components. The results we obtained are in the same order of magnitude as the ones obtained by Engberg and Frank (2011), who tested myoglobin diffusion through poly (ethylene glycol) hydrogels and Carvalho et al. (2008) who tested albumin diffusion through dextrin-vinyl acrylate hydrogels with different substitution degrees, confirming that the hydrogels we obtained allow a proper diffusion which can sustain encapsulated cell functions [60, 61].

Due to their macroscopic shape and mechanical properties discussed above, the hydrogels present potential use for a large spectrum of regenerative medical applications, particularly for stromal-like tissue engineering (skin and other parenchymal structures). Both gellan and pullulan, as crosslinking agents, provide the hydrogels with suitable properties for cell encapsulation which was further demonstrated through microscopic analysis and functional evaluation. Thus, light and fluorescent microscopy analysis performed on cell-populated hydrogels showed a good integration of encapsulated cells in the hydrogel structure (Fig. 4).

It is well known that the fibres have a very important structural and functional role, providing adhesion cues which are important for cell surviving and proliferation [62]. According to reported data, the morphology of cells encapsulated in polymers (either natural or synthetic), that do not present cues for cell adhesion, like alginate, carrageenan, PEG, PMBV/PVA, is rounded shaped although the cells appear to maintain their viability [63–65]. With hydrogels obtained using collagen, fibrin, hyaluronic acid and co-gels, adipose derived stem cells exhibit an elongated, fibroblast-like morphology [66]. Cell shape is influenced not only by the presence of adhesion cues but also by matrix stiffness as it was noted by Stowers et al. [67]; their study showed that matrix stiffening determines a predominantly rounded cell morphology, with differences between 2D and 3D culture. The elongated morphology of the cells encapsulated in the hydrogels we obtained (Fig. 5) is a result of their fibrous structure and reduced stiffness influenced directly by their composition.

A slight difference between the two types of hydrogels could be observed in respect to cell morphology especially after a longer time of culture. In the hydrogels crosslinked with partially oxidised gellan the cells are more elongated, this observation being correlated with those presented in the histological sections from Fig. 6.

The biological performance of the gellan-crosslinked sample was proved through *in vivo* evaluation which demonstrates the absence of any inflammatory response in the implantation area. The lymphocytes, neutrophil leucocytes, eosinophils, macrophages or giant cells, markers of inflammation, allergic reaction or foreign body reaction are not present at the implantation site of the obtained hydrogels, as shown in Fig. 9.

Functional evaluation of the hydrogels was assessed by encapsulating ovarian stromal cells. Theca-interstitial cells are active secretory cells from ovarian stroma that functionally interact with epithelial granulosa cells in order to convert androstenedione to estradiol by their specific aromatase activity, according to "two-cell two-hormone theory" [68].

According to Magoffin, theca-interstitial cells display a fibroblast-like morphology, with small lipid vesicles in the cytoplasm [69]. Unlike theca-interstitial cells, 2D cultured granulosa cells show a polygonal morphology, typical for epithelial cells. In this study, both types of cells (with known specific morphology) were isolated. The proliferation of granulosa cells was slower than for theca-interstitial cells, with a tendency to form clusters on the culture surface.

The intercellular cooperation (in 3D co-culture conditions of the oxidised polysaccharide-crosslinked hydrogels), was proved by estradiol production of granulosa cells after medium supplementation with FSH and LH (the two pituitary hormones that induce androstenedione formation in the theca cells (LH) on one hand, and aromatase activation in the granulosa cells (FSH) in other hand). E2 (17β-estradiol) is the main blood circulating isoform of estradiol with a molecular mass of 272.3 Da, having two hydroxyl groups. Blood circulating estradiol is bound to low-weight sex hormone-binding glycoproteins (with a molecular mass around 45 kDa) and serum albumin.

Comparing results obtained for the two hydrogels and 2D (Table 5) control it was concluded that the obtained matrices do not obstruct the release of small steroid hormone molecules. The functional concept demonstrates the possibility to apply these hydrogels as secretory stromal tissue (ovary for example) or as low-weight steroid hormone biological carriers.

The results regarding estradiol secretion are very similar to those obtained by Sittadjody et al. [70] on alginate microencapsulation, with the difference that the hydrogels assembled from native ECM components, as those presented in this paper, express advantages in terms of cell morphology, adhesion and intercellular interaction.

The freezing-thawing of the hydrogels with encapsulated cells showed that thawed cell-populated hydrogels ensure the maintenance of cell viability and proliferation, morphology preservation and all other hydrogel's characteristics i.e. physical integrity, transparency and handling properties. The continuous proliferation of the cells inside

the thawed hydrogels, as seen in Fig. 10, indicates the absence of a potentially cytotoxic effect of DMSO used as cryoprotective agent. The high cell viability may be the complex protective action of FBS as cryoprotective medium along with hydrogel composition. Thus, according to reported data, the cells cryopreserved using sodium hyaluronate express increased membrane integrity and the preservation of cell adhesion molecules due to an intracellular cryoprotective action and antioxidant effect [71–74]. The mechanisms of cryoprotection and functional analysis of the thawed constructs must be further evaluated.

As final conclusions, this paper demonstrates the possibility to obtain a bioactive stromal tissue using natural and biologically safe compounds, with no contribution of synthetic crosslinkers and cytotoxic procedures. Two polysaccharides, gellan and pullulan have been tested as crosslinkers for obtaining a stroma-like tissue based on ECM macromolecules, polysaccharides and specialised cells. Hence, fibrillary atelocollagen, NaHyal and partially oxidised polysaccharides (as crosslinking agents) in a mass ratio of 26: 1: 5 conducted to adequate cell embedding. Both gellan-crosslinked and pullulan-crosslinked hydrogels display very similar properties regarding low-weight molecular diffusion, cell viability and intercellular communication. A slight difference between the two types of hydrogels was recorded with regard to cell morphology and is correlated with hydrogel stiffness. The smaller pullulan molecules produce hydrogels with higher stiffness which determines a less elongated cell shape compared to larger gellan molecules, both polysaccharides being appropriate for two potentially different stromal environments. When implanted *in vivo,* the hydrogels do not trigger any inflammatory responses and integrate into the native tissue, giving promising perspectives as tissue replacement constructs. Molecule diffusion to and from encapsulated cells demonstrates that the porous architecture of the hydrogels, provided by the fibrillar structure, allows adequate cell–cell and cell–matrix signalling. The cell-hydrogel system can be cryopreserved using a simple and low-cost method, with a high rate of cell viability and macroscopic properties maintenance after thawing. These later arguments recommend the hydrogels as potentially ready-to-use artificial bioactive stromal tissue or as carriers for secretory cells.

Compliance with ethical standards

Conflict of interests The authors have no financial conflict of interests.

Ethical statement This study was approved by the Ethical Committee of Grigore T. Popa University of Medicine and Pharmacy of Iasi registered on 13 June 2016 for the submitted research No. PN-III-P2-2.1-PED-2016-1230.

References

1. McGettrick HM, Butler LM, Buckley CD, Rainger GE, Nash GB. Tissue stroma as a regulator of leukocyte recruitment in inflammation. J Leukoc Biol. 2012;91:385–400.
2. Shen K, Luk S, Hicks DF, Elman JS, Bohr S, Iwamoto Y, et al. Resolving cancer–stroma interfacial signalling and interventions with micropatterned tumour–stromal assays. Nat Commun. 2014;5:5662.
3. Deng C, Zhang P, Vulesevic B, Kuraitis D, Li F, Yang AF, et al. A collagen-chitosan hydrogel for endothelial differentiation and angiogenesis. Tissue Eng Part A. 2010;16:3099–109.
4. Sargeant TD, Desai AP, Banerjee S, Agawu A, Stopek JB. An in situ forming collagen-PEG hydrogel for tissue regeneration. Acta Biomater. 2012;8:124–32.
5. Koshy ST, Ferrante TC, Lewin SA, Mooney DJ. Injectable, porous, and cell-responsive gelatin cryogels. Biomaterials. 2014;35:2477–87.
6. Sarker B, Singh R, Silva R, Roether JA, Kaschta J, Detsch R, et al. Evaluation of fibroblasts adhesion and proliferation on alginate-gelatin crosslinked hydrogel. PLoS ONE. 2014;9:e107952.
7. Nicodemus GD, Bryant SJ. Cell encapsulation in biodegradable hydrogels for tissue engineering applications. Tissue Eng Part B Rev. 2008;14:149–65.
8. Itami S, Yasuda K, Yoshida Y, Matsui C, Hashiura S, Sakai A, et al. Co-culturing of follicles with interstitial cells in collagen gel reproduce follicular development accompanied with theca cell layer formation. Reprod Biol Endocrinol. 2011;9:159.
9. Geckil H, Xu F, Zhang X, Moon S, Demirci U. Engineering hydrogels as extracellular matrix mimics. Nanomedicine (London, England). 2010;5:469–84.
10. Collin EC, Grad S, Zeugolis DI, Vinatier CS, Clouet JR, Guicheux JJ, et al. An injectable vehicle for nucleus pulposus cell-based therapy. Biomaterials. 2011;32:2862–70.
11. Chung C, Lampe KJ, Heilshorn SC. Tetrakis(hydroxymethyl) phosphonium chloride as a covalent cross-linking agent for cell encapsulation within protein-based hydrogels. Biomacromol. 2012;13:3912–6.
12. Davis NE, Ding S, Forster R, Pinkas DM, Barron AE. Modular enzymatically crosslinked protein polymer hydrogels for in situ gelation. Biomaterials. 2010;31:7288–97.
13. Nichol JW, Koshy S, Bae H, Hwang CM, Yamanlar S, Khademhosseini A. Cell-laden microengineered gelatin methacrylate hydrogels. Biomaterials. 2010;31:5536–44.
14. Hutson CB, Nichol JW, Aubin H, Bae H, Yamanlar S, Al-Haque S, et al. Synthesis and characterization of tunable poly(ethylene glycol): gelatin methacrylate composite hydrogels. Tissue Eng Part A. 2011;17:1713–23.
15. Ghidoni I, Chlapanidas T, Bucco M, Crovato F, Marazzi M, Vigo D, et al. Alginate cell encapsulation: new advances in reproduction and cartilage regenerative medicine. Cytotechnology. 2008;58:49–56.
16. Park H, Woo EK, Lee KY. Ionically cross-linkable hyaluronate-based hydrogels for injectable cell delivery. J Control Release. 2014;196:146–53.
17. Mazzitelli S, Borgatti M, Breveglieri G, Gambari R, Nastruzzi C. Encapsulation of eukaryotic cells in alginate microparticles: cell signaling by TNF-alpha through capsular structure of cystic fibrosis cells. J Cell Commun Signal. 2011;5:157–65.
18. Wilson JL, Najia MA, Saeed R, McDevitt TC. Alginate encapsulation parameters influence the differentiation of microencapsulated embryonic stem cell aggregates. Biotechnol Bioeng. 2014;111:618–31.

19. Tang Y, Sun J, Fan H, Zhang X. An improved complex gel of modified gellan gum and carboxymethyl chitosan for chondrocytes encapsulation. Carbohydr Polym. 2012;88:46–53.
20. Dahlmann J, Krause A, Moller L, Kensah G, Mowes M, Diekmann A, et al. Fully defined in situ cross-linkable alginate and hyaluronic acid hydrogels for myocardial tissue engineering. Biomaterials. 2013;34:940–51.
21. Bouhadir KH, Lee KY, Alsberg E, Damm KL, Anderson KW, Mooney DJ. Degradation of partially oxidized alginate and its potential application for tissue engineering. Biotechnol Prog. 2001;17:945–50.
22. Xu Y, Li L, Wang H, Yu X, Gu Z, Huang C, et al. In vitro cytocompatibility evaluation of alginate dialdehyde for biological tissue fixation. Carbohydr Polym. 2013;92:448–54.
23. Geng XH, Yuan L, Mo XM. Oxidized dextran/amino gelatin/hyaluronic acid semi-interpenetrating network hydrogels for tissue engineering application. Adv Mater Res. 2013;627:745–50.
24. Geng X, Mo X, Fan L, Yin A, Fang J. Hierarchically designed injectable hydrogel from oxidized dextran, amino gelatin and 4-arm poly(ethylene glycol)-acrylate for tissue engineering application. J Mater Chem. 2012;22:25130–9.
25. Lisman A, Butruk B, Wasiak I, Ciach T. Dextran/Albumin hydrogel sealant for Dacron(R) vascular prosthesis. J Biomater Appl. 2014;28:1386–96.
26. Zhang X, Yang Y, Yao J, Shao Z, Chen X. Strong collagen hydrogels by oxidized dextran modification. ACS Sustain Chem Eng. 2014;2:1318–24.
27. Dias GJ, Peplow PV, Teixeira F. Osseous regeneration in the presence of oxidized cellulose and collagen. J Mater Sci Mater Med. 2003;14:739–45.
28. Rinaudo M. Periodate oxidation of methylcellulose: characterization and properties of oxidized derivatives. Polymers. 2010;2:505.
29. Gong Y, Wang C, Lai RC, Su K, Zhang F, Wang D-A. An improved injectable polysaccharide hydrogel: modified gellan gum for long-term cartilage regenerationin vitro. J Mater Chem. 2009;19:1968–77.
30. Tan H, Chu CR, Payne KA, Marra KG. Injectable in situ forming biodegradable chitosan-hyaluronic acid based hydrogels for cartilage tissue engineering. Biomaterials. 2009;30:2499–506.
31. Liu LS, Thompson AY, Heidaran MA, Poser JW, Spiro RC. An osteoconductive collagen/hyaluronate matrix for bone regeneration. Biomaterials. 1999;20:1097–108.
32. Chan BP, Hui TY, Wong MY, Yip KH, Chan GC. Mesenchymal stem cell-encapsulated collagen microspheres for bone tissue engineering. Tissue Eng Part C Methods. 2010;16:225–35.
33. Hesse E, Hefferan TE, Tarara JE, Haasper C, Meller R, Krettek C, et al. Collagen type I hydrogel allows migration, proliferation and osteogenic differentiation of rat bone marrow stromal cells. J Biomed Mater Res A. 2010;94:442–9.
34. Achilli M, Mantovani D. Tailoring mechanical properties of collagen-based scaffolds for vascular tissue engineering: the effects of pH, temperature and ionic strength on gelation. Polymers. 2010;2:664.
35. Oliveira JT, Martins L, Picciochi R, Malafaya PB, Sousa RA, Neves NM, et al. Gellan gum: a new biomaterial for cartilage tissue engineering applications. J Biomed Mater Res A. 2010;93:852–63.
36. Smith AMSRM, Perrie Y, Harris JJ. An initial evaluation of gellan gum as a material for tissue engineering applications. J Biomater Appl. 2007;22:241–54.
37. Tsaryk R, Silva-Correia J, Oliveira JM, Unger RE, Landes C, Brochhausen C, et al. Biological performance of cell-encapsulated methacrylated gellan gum-based hydrogels for nucleus pulposus regeneration. J Tissue Eng Regen Med. 2014.
38. Bulman SE, Coleman CM, Murphy JM, Medcalf N, Ryan AE, Barry F. Pullulan: a new cytoadhesive for cell-mediated cartilage repair. Stem Cell Res Ther. 2015;6:34.
39. Li X, Xue W, Liu Y, Li W, Fan D, Zhu C, et al. HLC/pullulan and pullulan hydrogels: their microstructure, engineering process and biocompatibility. Mater Sci Eng C Mater Biol Appl. 2016;58:1046–57.
40. Bae H, Ahari AF, Shin H, Nichol JW, Hutson CB, Masaeli M, et al. Cell-laden microengineered pullulan methacrylate hydrogels promote cell proliferation and 3D cluster formation. Soft Matter. 2011;7:1903–11.
41. Hughes CS, Postovit LM, Lajoie GA. Matrigel: a complex protein mixture required for optimal growth of cell culture. Proteomics. 2010;10:1886–90.
42. Caliari SR, Burdick JA. A practical guide to hydrogels for cell culture. Nat Meth. 2016;13:405–14.
43. Pravdyuk AI, Petrenko YA, Fuller BJ, Petrenko AY. Cryopreservation of alginate encapsulated mesenchymal stromal cells. Cryobiology. 2013;66:215–22.
44. Malpique R, Osorio LM, Ferreira DS, Ehrhart F, Brito C, Zimmermann H, et al. Alginate encapsulation as a novel strategy for the cryopreservation of neurospheres. Tissue Eng Part C Methods. 2010;16:965–77.
45. Wang X, Paloheimo K-S, Xu H, Liu C. Cryopreservation of cell/hydrogel constructs based on a new cell-assembling technique. J Bioact Compat Polym. 2010;25:634–53.
46. Ahmad HF, Sambanis A. Cryopreservation effects on recombinant myoblasts encapsulated in adhesive alginate hydrogels. Acta Biomater. 2013;9:6814–22.
47. Luca A, Maier V, Maier SS, Butnaru M, Danu M, Ibanescu C, et al. Biomacromolecular-based ionic-covalent hydrogels for cell encapsulation: the atelocollagen—Oxidized polysaccharides couples. Carbohydr Polym. 2017;169:366–75.
48. Freshney RI. Culture of animal cells: a manual of basic techniques and specialized applications. 6th ed. Hoboken: Wiley; 2010.
49. Tingen CM, Kiesewetter SE, Jozefik J, Thomas C, Tagler D, Shea L, et al. A macrophage and theca cell-enriched stromal cell population influences growth and survival of immature murine follicles in vitro. Reproduction. 2011;141:809–20.
50. Wong VW, Rustad KC, Galvez MG, Neofytou E, Glotzbach JP, Januszyk M, et al. Engineered pullulan-collagen composite dermal hydrogels improve early cutaneous wound healing. Tissue Eng Part A. 2011;17:631–44.
51. Staunton JR, Doss BL, Lindsay S, Ros R. Correlating confocal microscopy and atomic force indentation reveals metastatic cancer cells stiffen during invasion into collagen I matrices. Sci Rep. 2016;6:19686.
52. Guha D, Chakraborty B, Dutta HS. Computer, Communication and Electrical Technology: Proceedings of the International Conference on Advancement of Computer Communication and Electrical Technology (ACCET 2016), West Bengal, India, 21–22 October 2016: CRC Press; 2017.
53. Ji L, de Pablo JJ, Palecek SP. Cryopreservation of adherent human embryonic stem cells. Biotechnol Bioeng. 2004;88:299–312.
54. Sambu S, Xu X, Schiffer HA, Cui ZF, Ye H. RGDS-fuctionalized alginates improve the survival rate of encapsulated embryonic stem cells during cryopreservation. Cryo Lett. 2011;32:389–401.
55. Banerjee A, Arha M, Choudhary S, Ashton RS, Bhatia SR, Schaffer DV, et al. The influence of hydrogel modulus on the proliferation and differentiation of encapsulated neural stem cells. Biomaterials. 2009;30:4695–9.
56. Hwang PY, Chen J, Jing L, Hoffman BD, Setton LA. The role of extracellular matrix elasticity and composition in regulating the

nucleus pulposus cell phenotype in the intervertebral disc: a narrative review. J Biomech Eng. 2014;136:0210101–9.
57. Johnson AW, Harley B. Mechanobiology of cell-cell and cell-matrix interactions. New York: Springer; 2011.
58. Markert CD, Guo X, Skardal A, Wang Z, Bharadwaj S, Zhang Y, et al. Characterizing the micro-scale elastic modulus of hydrogels for use in regenerative medicine. J Mech Behav Biomed Mater. 2013;27:115–27.
59. Levesque SG, Lim RM, Shoichet MS. Macroporous interconnected dextran scaffolds of controlled porosity for tissue-engineering applications. Biomaterials. 2005;26:7436–46.
60. Engberg K, Frank CW. Protein diffusion in photopolymerized poly(ethylene glycol) hydrogel networks. Biomed Mater. 2011;6:055006.
61. Carvalho JM, Coimbra MA, Gama FM. New dextrin-vinylacrylate hydrogel: studies on protein diffusion and release. Carbohydr Polym. 2009;75:322–7.
62. Beachley V, Wen X. Polymer nanofibrous structures: fabrication, biofunctionalization, and cell interactions. Prog Polym Sci. 2010;35:868–92.
63. Rocha PM, Santo VE, Gomes ME, Reis RL, Mano JF. Encapsulation of adipose derived stem cells and transforming growth factor-b1 in carrageenan-based hydrogels for cartilage tissue engineering. J Bioact Compat Polym. 2011;26:493–507.
64. Hassan W, Dong Y, Wang W. Encapsulation and 3D culture of human adipose-derived stem cells in an in situ crosslinked hybrid hydrogel composed of PEG-based hyperbranched copolymer and hyaluronic acid. Stem Cell Res Ther. 2013;4:32.
65. Ishihara K, Xu Y, Konno T. Cytocompatible hydrogel composed of phospholipid polymers for regulation of cell functions. In: Kunugi S, Yamaoka T, editors. Polymers in Nanomedicine. Berlin: Springer; 2011. p. 141–65.
66. Park H, Karajanagi S, Wolak K, Aanestad J, Daheron L, Kobler JB, et al. Three-dimensional hydrogel model using adipose-derived stem cells for vocal fold augmentation. Tissue Eng Part A. 2010;16:535–43.
67. Stowers RS, Allen SC, Suggs LJ. Dynamic phototuning of 3D hydrogel stiffness. Proc Natl Acad Sci U S A. 2015;112:1953–8.
68. Liu YX, Hsueh AJ. Synergism between granulosa and theca-interstitial cells in estrogen biosynthesis by gonadotropin-treated rat ovaries: studies on the two-cell, two-gonadotropin hypothesis using steroid antisera. Biol Reprod. 1986;35:27–36.
69. Magoffin D. Ovarian granulosa and theca cells. In: Bidey S, editor. Endocrine Cell culture. Cambridge: Cambridge University Press; 1998. p. 22–5.
70. Sittadjody S, Saul JM, Joo S, Yoo JJ, Atala A, Opara EC. Engineered multilayer ovarian tissue that secretes sex steroids and peptide hormones in response to gonadotropins. Biomaterials. 2013;34:2412–20.
71. Peer D, Florentin A, Margalit R. Hyaluronan is a key component in cryoprotection and formulation of targeted unilamellar liposomes. Biochim Biophys Acta. 2003;1612:76–82.
72. Ujihira M, Iwama A, Aoki M, Aoki K, Omaki S, Goto E, et al. Cryoprotective effect of low-molecular-weight hyaluronan on human dermal fibroblast monolayers. Cryo Lett. 2010;31:101–11.
73. Iwama A, Yamada C, Uchida K, Ujihira M. Pre-incubation with hyaluronan reduces cellular damage after cryopreservation in densely cultured cell monolayers. Biomed Mater Eng. 2014;24:1497–506.
74. Turner RA, Mendel G, Wauthier E, Barbier C, Reid LM. Hyaluronan-supplemented buffers preserve adhesion mechanisms facilitating cryopreservation of human hepatic stem/progenitor cells. Cell Transplant. 2012;21:2257–66.